Processing and Application of Ceramics 14 [1] (2020) 63–70
https://doi.org/10.2298/PAC2001063G

Silicon nitride with titania, calcia and silica additives for orthopaedic applications

Cecilia C. Guedes-Silva[1,*], Andrea C.D. Rodas[2], Flávio M.S. Carvalho[3], Olga Z. Higa[1], Thiago S. Ferreira[1]

[1]*Nuclear and Energy Research Institute, São Paulo, SP, 05508-000, Brazil*
[2]*Center of Engineering, Modeling and Applied Social Sciences, Federal University of ABC, São Bernardo do Campo, SP, 09606-045, Brazil*
[3]*Geoscience Institute, University of São Paulo, SP, 05508-080, Brazil*

Received 15 August 2019; Received in revised form 27 December 2019; Accepted 29 February 2020

Abstract

Titanium, silicon and calcium ions have demonstrated positive effects in bone healing. Therefore, this paper investigates the densification, mechanical properties and in vitro biological behaviour of TiO_2, together with SiO_2 and CaO, on silicon nitride ceramics to be used in clinical applications. The results revealed that the sintered samples reached high values of relative density and fracture toughness, non-cytotoxicity as well as good ability to promote cell proliferation and form a layer of carbonated hydroxyapatite on their surfaces, after immersion in simulated body fluid. The sample with the highest amount of TiO_2 reached the highest value of relative density and the best results of cell proliferation and fracture toughness, indicating the great potential to be explored by in vivo experiments for later application as intervertebral devices.

Keywords: *Si_3N_4, titania/calcia/silica additives, bioceramics, mechanical properties, cell proliferation*

I. Introduction

Pain in the back is a health problem usually related to musculoskeletal injuries and degenerative diseases [1]. Although many problems can be treated by physiotherapy sessions, medication and rest, sometimes these methods are not enough, requiring surgical interventions for rehabilitation of the patient [2]. The successful spine surgeries are those using interbody cages [3] because they can promote lower postoperative pain, shorter hospitalization time, fewer complications and higher fusion rates than the fusion surgeries using autogenous bone exclusively [4].

The intervertebral devices incorporate the bone graft, preserve the disc height and provide immediate stability of the operated segment. They are usually made of titanium, titanium alloys or PEEK (polyether ether ketone), and may have different sizes and shapes, depending on the patient's anatomy [5,6]. Titanium devices were introduced in the 90's owing to low density, high corrosion resistance, good osseointegration and bone adhesion. However, this material exhibits high elastic modulus and poor imaging features. On the other hand, PEEK is a non- cytotoxic, radiolucent material with an elastic modulus close to the cortical bone [6–8], but it does not adequately integrate to the neighbouring bone and can develop connective tissue at the interface, causing micro movements and implant failures [9,10].

In this context, silicon nitride has appeared as an alternative material to make spinal devices [11]. The good biologic response of silicon nitride is evidenced by the high flexural strength, non-cytotoxicity [12] and ability to promote intense bone growth [13,14]. Moreover, this ceramics is a partially radiolucent material while it presents a high antibacterial function and better connection between living bone than titanium and PEEK implants [15,16].

However, sintering aids must be carefully selected to obtain silicon nitride components with propitious mechanical properties and adequate biological response. A good way to select these additives is considering the therapeutic effect of their ions. Ions as calcium and silicon, for example, play an important role in angiogene-

* Corresponding author: tel: +55 11 3133 9394,
e-mail: *cecilia.guedes@ipen.br*

sis, growth and mineralization of bone tissue, inducing the precipitation of hydroxyapatite on implants surfaces and improving the collagen synthesis in osteoblasts [17–20]. A previous work [21] focused on researching the effect of SiO_2 and CaO additions on silicon nitride ceramics, demonstrating the potential of these oxides to obtain silicon nitride components for biomedical applications [21].

As titanium has antitumour properties and favours cell response [22,23], the present work aims to evaluate the effect of different contents of TiO_2, SiO_2 and CaO on sintering, microstructure, mechanical properties and biological response of silicon nitride ceramics for use as prosthetic components.

II. Experimental details

2.1. Sample preparation

Silicon nitride based ceramics were prepared using: commercial α-Si_3N_4 powders (UBE, SN-E10), SiO_2 (quartz, 99.9% purity, Sigma-Aldrich), $CaCO_3$ (P.A., Vetec) and TiO_2 (anatase, 99.9% purity, Sigma-Aldrich). As the temperature of liquid formation is one of the most important factors that favours the liquid sintering of silicon nitride, the amount of each additive was defined so that the compositions (Table 1) could reach liquidus temperatures between 1350 and 1500 °C in the CaO-TiO_2-SiO_2 phase diagram described by DeVries *et al.* [24]. Next, the powders of the desired compositions were ground for 4 h in a high-energy mill at 400 rpm using isopropanol as the solvent and Si_3N_4 balls as media. After drying using a rotary evaporator, the powders were compacted by uniaxial (50 MPa) and cold isostatic (200 MPa) pressing. Due to the decomposition temperature of Si_3N_4 at atmospheric pressure at about 1840 °C [25], the pellets were pressureless sintered at 1815 °C for 1 h using a graphite resistance furnace (Thermal Technology) in a high purity nitrogen atmosphere. The samples were finished with a diamond wheel to achieve a surface roughness between 0.3 and 0.4 μm.

2.2. Structural characterization

The density of the sintered samples was determined by the Archimedes' method using distilled water, while the relative density was calculated according to the rule of mixtures, considering the theoretical density of the starting powders. Crystalline phases after sintering were identified by X-ray diffraction (XRD) with a Brucker D8 X-ray diffractometer using CuKα radiation. The TiN/β-Si_3N_4 ratios were determined by Rietveld method using Topas Academic V5 software [26]. The microstructural analysis was performed on the polished and plasma-etched (using SF_6:O_2) surfaces by scanning electron microscopy (SEM) using JEOL JSM6701F FEG-SEM equipped with an energy dispersive spectroscope (EDS). Grain size was estimated using ImageJ as image analysis software [27].

2.3. Hardness and fracture toughness

Vickers indentations were performed on the ground and polished disc-shaped samples (10 mm in diameter and 1.0 mm in thickness) using a hardness tester (Buhler VH1150 Durometer), load of 100 N and loading time of 15 s at room temperature. The lengths of the impression diagonals and surface cracks were measured immediately after indentations to determine the fracture toughness (K_{IC}) by the equation of Anstis *et al.* [28] (prior to examination, the samples were sputter coated with Au):

$$K_{IC} = 0.016\left(\frac{E}{H_v}\right)^{1/2}\frac{P}{c^{2/3}} \quad (1)$$

where H_v is the Vickers hardness, P is the applied load, c is the half-length of radial crack and E the Young's modulus (300 GPa) [29].

2.4. Acellular biological response

In vitro reactivity tests were performed by immersing the samples in simulated body fluid (SBF) solution at pH = 7.20 and 37 °C. pH measurements of the solution containing each sample were performed every 84 h. After 14 days, the samples were washed with water, dried at 37 °C and their surfaces were analysed using scanning electron microscopes (Philips XL30 SEM and JEOL JSM6701F FEG-SEM) and EDS.

2.5. Cellular response

Tests of cytotoxicity were performed by indirect method according to ISO 10993-5, using mouse fibroblasts cells (Balb/c, ATCC). Extracts of each sample were obtained by incubating them in the culture medium (DMEM, Gibco) at 37 °C for 72 h under sterile conditions. At the end of the incubations, the extracts were transferred to 96-well plates with a confluent monolayer of Balb/c cells (2×10^4 cells per well). After 24 h, the extracts were replaced by culture medium containing MTS vital dye (Promega). This dye reacts with living cells to form a coloured compound that can be quantified by measuring the absorbance at 490–500 nm. Aliquots of the sterile media were used as a control and the optical density of the wells was used to calculate cell viability.

For cell proliferation study, human osteoblast-like cells (MG63, ATCC) were grown in Minimum Essential

Table 1. Composition of the prepared samples

Sample	Si_3N_4 [wt.%]	SiO_2 [wt.%]	TiO_2 [wt.%]	CaO [wt.%]
SSCT-1	90.0	1.0	5.0	4.0
SSCT-2	90.0	2.5	3.5	4.0
SSCT-3	90.0	3.0	3.0	4.0
SSCT-4	90.0	4.0	2.5	3.5

Table 2. Densities and apparent porosity of the samples

Sample	Apparent density [g/cm^3]	Relative density [%TD]	Apparent porosity [%]
SSCT-1	3.131 ± 0.006	97.56 ± 0.18	0.32 ± 0.11
SSCT-2	3.050 ± 0.013	95.64 ± 0.36	1.01 ± 0.48
SSCT-3	3.052 ± 0.008	95.82 ± 0.24	0.78 ± 0.20
SSCT-4	3.040 ± 0.020	96.32 ± 0.29	0.93 ± 0.55

Medium (MEM, Gibco) supplemented with 10% fetal bovine serum (Cultilab) and 1% antibiotic/antimycotic solution (Gibco) at 37 °C in 5% CO_2 and 100% humidity. After confluence, the cells were trypsinized with trypsin 0.05%-EDTA 0.02% solution (Sigma). The cells were cultured with the samples for 3, 7 and 14 days. Before seeding, cleaned and sterilized silicon nitride samples were placed in 24-well culture plates and 2×10^4 cells per sample were added and incubated at 37 °C. The culture medium was changed every 3 days. After each seeding period, MTS (Promega) reagent was added to culture medium, standardized as 500 µl for each sample. After 2 h incubation, supernatant aliquots were transferred to a 96-well plate and the absorbance at 492 nm was read using an Elisa Plate Reader. The samples were dehydrated, fixed in formaldehyde and coated with Au to be analysed by scanning electron microscopy (SEM, Hitachi TM 3000 microscope).

III. Results and discussion

The densities and apparent porosity of the studied materials are given in Table 2. All silicon nitride samples reached high relative densities and low apparent porosities after sintering at 1815 °C for 1 h. It means that the oxides (SiO_2, CaO and TiO_2) formed a liquid phase with adequate characteristics (viscosity, solubility, wetting, etc.) to promote the sintering of silicon nitride and its densification. However, the SSCT-1 sample had a slightly higher value of apparent density and the lowest value of porosity. It indicates that the presence of TiO_2 in the Si_3N_4 ceramics played a great role during the densification of silicon nitride using the pressureless sintering technique. Besides Ca ions from additions of CaO, Ti ions tend to increase the disruption of the silica network [30], decreasing the liquid viscosity during the sintering process and improving the densification.

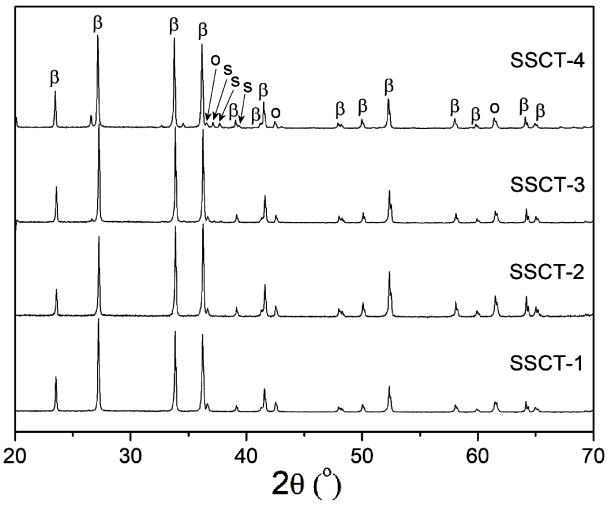

Figure 1. X-ray diffraction patterns of silicon nitride samples (β - Si_3N_4, o - TiN, s - Si_2ON_2)

The efficient performance of the used additives is also verified by XRD diffractograms shown in Fig. 1 that demonstrate the total $\alpha \rightarrow \beta$-Si_3N_4 transformation after 1 h of sintering for all samples. This behaviour was similar to that found using only SiO_2 and CaO as sintering aids for silicon nitride [21], showing that TiO_2 did not damage the liquid phase characteristics needed to promote the dissolution of the α-Si_3N_4 phase.

Beside β-Si_3N_4, identified as the major crystalline phase in the samples (Fig. 1), TiN was found as the second phase owing to reactions between Si_3N_4 and TiO_2 [31] as follows:

$$6\,TiO_2 + 4\,Si_3N_4 \rightarrow 6TiN + 12\,SiO(g) + 5\,N_2(g) \quad (2)$$

$$6\,TiO_2 + 2\,Si_3N_4 \rightarrow 6TiN + 6\,SiO(g) + N_2(g) \quad (3)$$

TiN/β-Si_3N_4 ratios calculated by Rietveld refinements from XRD data (Table 3) show that the content of TiN was increased with the initial concentration of TiO_2 in the samples. The formation of TiN phase is very interesting because its high electrical conductivity makes possible to manufacture biomedical devices by means of EDM (electrical discharge machining) which is able to produce complex parts with dimensional accuracy and great surface finish [32].

Table 3. TiN/Si_3N_4 ratios in the samples

Sample	TiN/β-Si_3N_4 ratio [wt.%]
SSCT-1	0.0456
SSCT-2	0.0283
SSCT-3	0.0265
SSCT-4	0.0222

The presence of Si_2ON_2 in the SSCT-2, SSCT-3 and SSCT-4 ceramics is also verified and it can be associated with the reaction $SiO_2 + Si_3N_4 \rightarrow 2\,Si_2ON_2$ [33] due to the high contents of SiO_2 in the samples.

Fig. 2 shows a SEM image of the SSCT-1 sample, representing the plasma-etched microstructure of the four studied samples. The samples developed similar microstructures with low porosity and elongated β-Si_3N_4 grains with the dispersant mean sizes determined as 0.66±0.45, 0.67±0.48, 0.67±0.47 and 0.67±0.40 µm for the SSCT-1, SSCT-2, SSCT-3 and SSCT-4 ceramics, respectively. Moreover, the β-Si_3N_4 grains are embed-

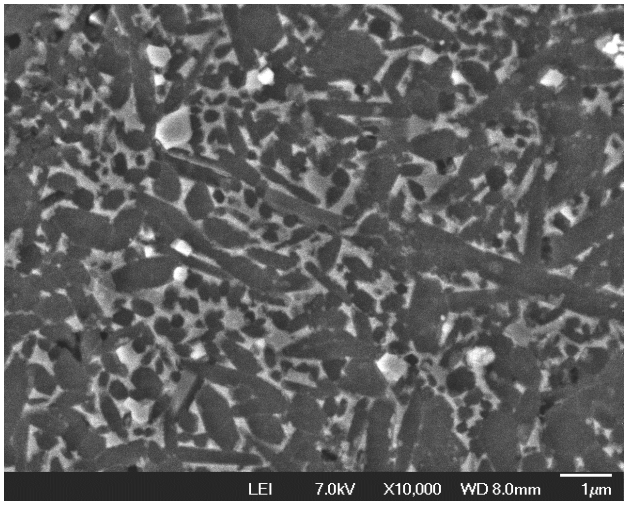

Figure 2. SEM micrograph of SSCT-1 sample

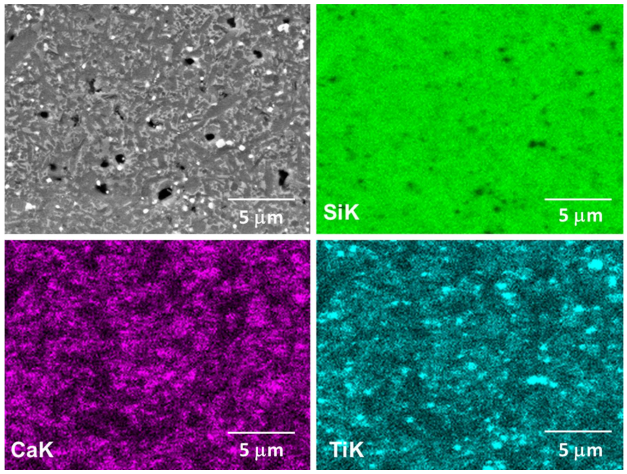

Figure 3. SEM image of SSCT-1 sample (a) and the element mapping images of Si (b), Ca (c) and Ti (d)

ded in the intergranular phase appearing in the image as light grey areas containing white particles.

A SEM image of the SSCT-1 sample with the EDS mapping images of Si, Ca and Ti are shown in Fig. 3. Figure 3b illustrates that silicon is distributed in both dark (β-Si_3N_4 grains) and light grey areas (intergranular phase). Calcium is rather present in the light grey areas while titanium is both in light grey and white areas. These results together with those of XRD (Fig. 1) demonstrate that the dark grey areas in Figs. 2 and 3a are the β-Si_3N_4 grains, the white areas are the TiN particles and the light grey areas are the intergranular phase that contains Si, Ca and Ti. This last phase is very likely an amorphous phase resulting from the cooling of the liquid formed by the oxides during the sintering process.

This kind of microstructure [34,35] plays a fundamental role in obtaining ceramics with good mechanical properties, mainly fracture toughness, important for preventing implant failures usually initiated by cracks during tasks in daily activities [36,37]. Here, values of fracture toughness around 6.0 MPa·m$^{1/2}$ were reached as shown in Table 4.

Table 4. Hardness (H_V) and fracture toughness (K_{IC})

Sample	H_V [GPa]	K_{IC} [MPa·m$^{1/2}$]
SSCT-1	12.65 ± 0.30	6.48 ± 0.52
SSCT-2	12.40 ± 0.37	6.14 ± 0.52
SSCT-3	12.27 ± 0.30	6.00 ± 0.62
SSCT-4	12.40 ± 0.32	5.52 ± 0.60

Also, it is noted (Table 4) that similar values of fracture toughness have been found for all samples. However, there is a tendency that higher content of titania in compositions increases the fracture toughness of the material. This trend may be due to the increased content of the TiN phase in the grain boundaries that is able to induce different toughening mechanisms, such as crack bridging, crack deflection and microcracking [37]. This is why TiN is often used as the second phase in silicon nitride composites.

Very similar values of hardness were found for the studied compositions, except for the SSCT-1 sample whose value was slightly higher than those reached in the others samples, probably due to its higher density (Table 2), i.e. lower porosity.

During the immersion in SBF, pH changes of the solutions were observed (Fig. 4) as an indication of the reactions proposed by Kokubo *et al.* [38]. After 84 h of immersion, the pH values increased for all solutions owing to the fast release of Ca^{2+}, Ti^{3+} or Ti^{4+} from the sample surfaces followed by the increased concentration of hydroxyl groups. These groups tend to react with the intergranular phase of the samples, producing acidic radicals in the form of silanols and decreasing the pH of the solutions. After 14 days of immersion, the pH of the solutions increased again and can be attributed to dissociation reactions that increase both amounts of hydroxyls and cations (coming from the samples) in SBF. In addition, it is possible to see in Fig. 4 the high pH variation reached by the SSCT-1 sample, which is probably due to the loss of the Si–O–Si network connectivity in the intergranular glassy phase with Ca and Ti as modifier cations [39]. This mechanism can introduce

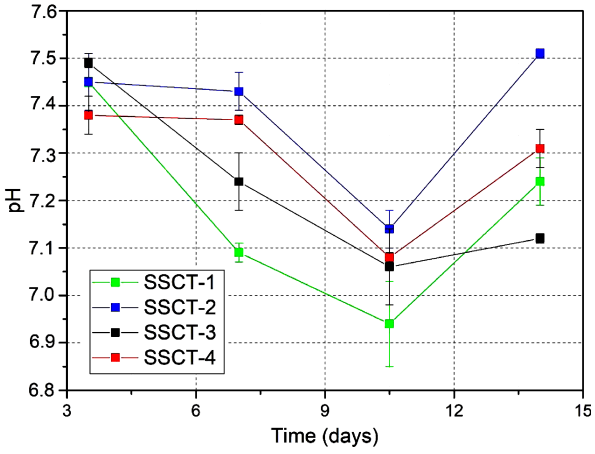

Figure 4. Variation of pH of the SBF solutions containing Si_3N_4 samples

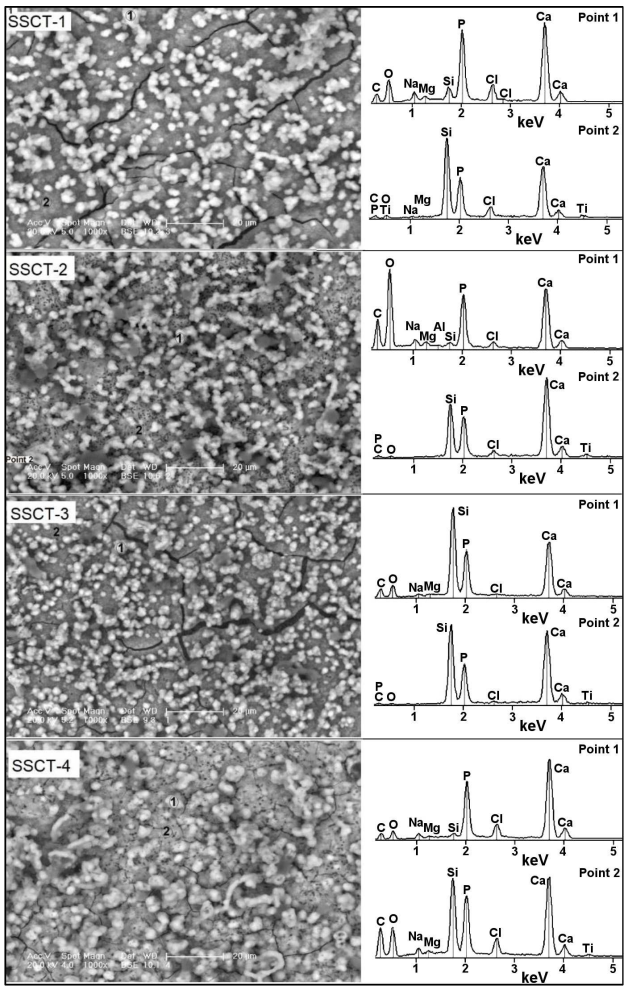

Figure 5. SEM images and EDS of samples surfaces after 14 days of immersion in SBF solution

non-bridging oxygen in the glass network favouring the reactions in SBF.

SEM images (Fig. 5) of the surfaces after 14 days of immersion in SBF reveal that a dense layer with mineral nodules was formed in all samples. Cracks are also present since they are the result of the drying process. The EDS analysis indicates that the layer consists of calcium phosphate (CaP) phase, also containing silicon, titanium, magnesium, potassium and other ions coming from the solution or the sample itself. The globular morphology of the nodules confirmed by FEG-SEM images (Fig. 6) together with the elemental analysis from EDS (Fig. 5) strongly suggests that the formed layer is carbonated hydroxyapatite (CHA). The formation of CHA on the samples after immersion in SBF is a great result for the application of materials as devices in spine arthrodesis. Surfaces like those studied in this work are very promising to have strong interaction with the newly formed bone besides favouring its rapid growth *in vivo*.

Figure 7 shows the cytotoxicity evaluation of the extracts obtained from each sample as previously described. It is noted that the samples exhibited no *in vitro* cytotoxicity effect and there was no significant difference in cell viability considering the four studied compositions.

The cellular behaviour of MG63 cells was investigated on the disks of the four silicon nitride samples (Fig. 8). It is observed that MG63 cells could proliferate on all substrates, indicating the positive influence of the doping, roughness and grain sizes of the samples. It is clear from Fig. 8 that the cells number increased with the seeding time, with cells forming a thick layer on the substrates after 14 days of culture. Cell adhesion and proliferation are a great demonstration of the bio-

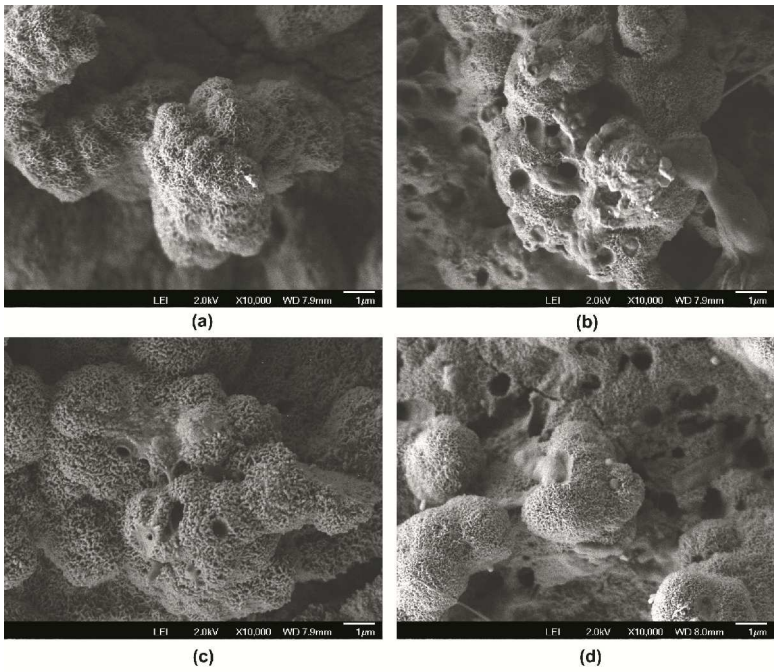

Figure 6. FEG-SEM images of the samples surfaces after 14 days of immersion in SBF: a) SSCT-1, b) SSCT-2, c) SSCT-3 and d) SSCT-4

compatibility of materials because these responses are involved in the healing and tissue integration processes *in vivo* [40].

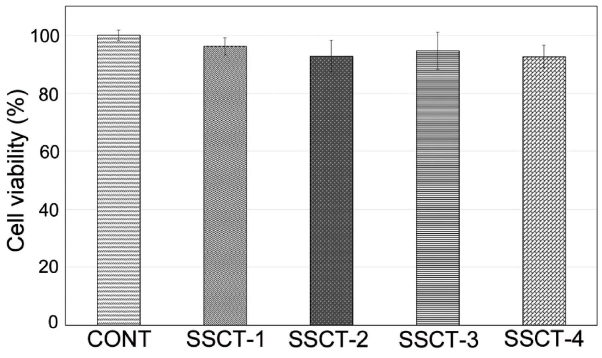

Figure 7. Cell toxicity of the control and the samples extracts determined by MTS assay in Balb/c cells

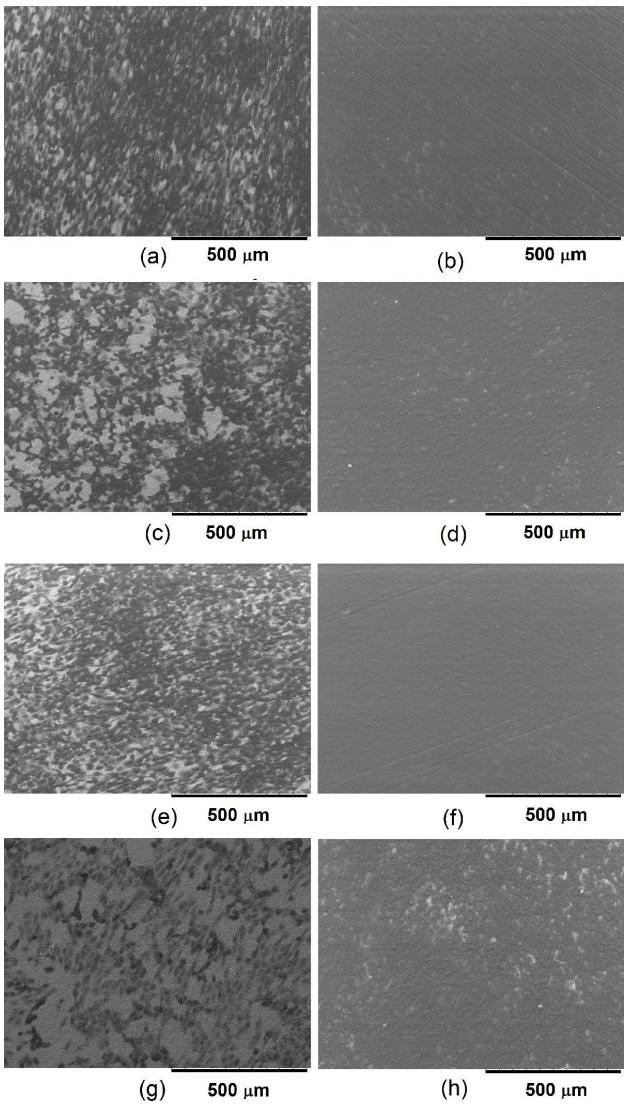

Figure 8. SEM images of the MG63 cells cultured on the silicon nitride samples surfaces: a) SSCT-1/7 days, b) SSCT-1/14 days, c) SSCT-2/7 days, d) SSCT-2/14 days, e) SSCT-3/7 days, f) SSCT-3/14 days, g) SSCT-4/7 days and h) SSCT-4/14 days

Moreover, during the cell culture, the effect of titanium on cell growth can be noted, since the sample with higher content of TiO_2 (SSCT-1) had the greater cell proliferation, demonstrated by the higher average values of absorbance (Fig. 9). Possibly, the higher amount of TiN and the great ability of these samples to form CHA on their surfaces as demonstrated by SBF tests, favours the protein adsorption on the material surface and the subsequent process of cell proliferation. This is because protein adsorption involved in cell interactions depends on factors such as pH and ionic composition of the solution, both influenced by the surface chemistry of the material [41].

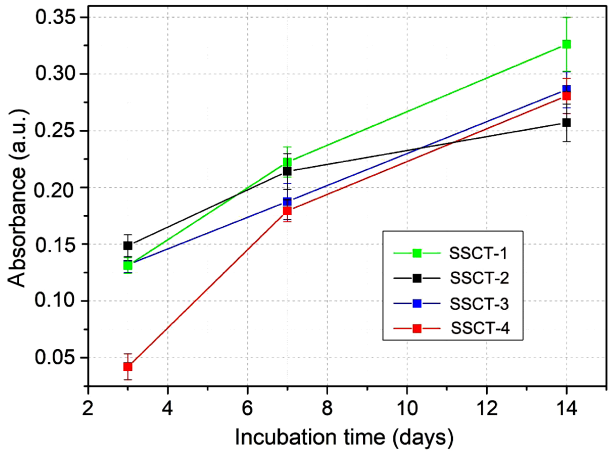

Figure 9. MTS assay at 3, 7 and 14 days of cell culture

The silicon nitride ceramics doped with titania, calcia and silica are promising for applications in the orthopaedics field. The results of densification, fracture toughness, reactivity in SBF, cytotoxicity as well as cell proliferation indicate that the materials tend to have high interaction with the host bone and perform their mechanical function properly when implanted *in vivo*. This behaviour is desirable for materials to be used as intervertebral devices, as it is a requirement for better fusion rates, height restoration and long-term stabilization [2,6]. Moreover, the studied materials present an important advantage of containing bioinorganic ions in their composition, i.e. titanium, calcium and silicon. The release of these ions into the body during *in vivo* implantation is expected to increase the osteoblasts proliferation while improving the balance between osteoclast and osteoblast activity, and the antibacterial function [17–19].

IV. Conclusions

Silicon nitride ceramics with titania, calcia and silica additives were prepared from corresponding commercial powders by sintering at 1815 °C for 1 h in a high purity nitrogen atmosphere. The used additives enabled production of silicon nitride ceramics with high relative density, absence of cytotoxicity and microstructures containing elongated grains of β-Si_3N_4. Increased contents of TiO_2 in the initial formulations promoted bet-

ter results of densification, fracture toughness, reactivity in SBF and *in vitro* cell proliferation. The presence of TiO_2 also favours crystallization of TiN phase in the grain boundaries, which may simplify the production of materials for the spine devices by using advance manufacturing methods such as electrical discharge machining.

Acknowledgments: The authors thank the Laboratory of Microscopy and Microanalysis. This research was funded by Fundação de Amparo à Pesquisa do Estado de São Paulo, grant number 2015/02265-7.

References

1. B. Karnath, "Clinical signs low of low back pain", *Hosp. Physician.*, **39** (2003) 39–44.
2. B.R. Whatley, X. Wen, "Intervertebral disc (IVD): Structure, degeneration, repair and regeneration", *Mater. Sci. Eng. C*, **32** (2012) 61–77.
3. J. Cadman, C. Sutterlin III, D. Dabirrahmani, R. Appleyard, " The importance of loading the periphery of the vertebral endplate", *J. Spine Surg.*, **2** (2016) 178–184.
4. S. Jain, A.E.M. Eltorai, R. Ruttiman, A.H. Daniels, "Advances in spinal interbody cages", *Orthop. Surg.*, **8** (2016) 278–284.
5. S.L. Blumenthal, D.D. Ohnmeiss, "Intervertebral cages for degenerative spinal diseases", *Spine*, **3** (2003) 301–309.
6. J.M. Toth, M. Wang, B.T. Estes, J.L. Scifert, H.B. Seim, A.S. Turner, "Polyetheretherketone as a biomaterial for spinal application", *Biomaterials*, **27** (2006) 324–334.
7. S.M., Kurtz, J.N. Devine, "PEEK biomaterials in trauma, orthopedic and spinal implants", *Biomaterials*, **28** (2007) 4845–4869.
8. H.J. Bruner, Y. Guan, N.F. Yoganandan, A. Pintar, D.J. Maiman, M.A. Slivka, "Biomechanics of polyaryletherketone rod composites and titanium rods for posterior lumbosacral instrumentation", *J. Neurosurg. Spine*, **13** (2010) 766–772.
9. E.R.G. Santos, D.G. Goss, R.K. Morcom, R.D. Fraser, "Radiologic assessment of interbody fusion using carbon fiber cages", *Spine*, **28** (2003) 997–1001.
10. N.K. Anjarwalla, R.K. Morcom, R.D. Fraser, "Supplementary stabilization with anterior lumbar intervertebral fusion – A radiologic review", *Spine*, **31** (2006) 1281–1287.
11. W.M. Rambo Jr., "Treatment of lumbar discitis using silicon nitride spinal spacers: A case series and literature review", *Int. J. Surg. Case Rep.*, **43** (2018) 61–68.
12. C.C. Guedes-Silva, O.Z. Higa, J.C. Bressiani, "Cytotoxic evaluation of silicon nitride-based ceramics", *Mater. Sci. Eng. C*, **24** (2004) 643–646.
13. C.C. Guedes-Silva, B. Konig Jr., M.J. Carbonari, M. Yoshimoto, S. Allegrini Jr., J.C. Bressiani, "Bone growth around silicon nitride implants – An evaluation by scanning electron microscopy", *Mater. Character.*, **9** (2008) 1339–1341.
14. C.C. Guedes-Silva, B. Konig Jr., M.J. Carbonari, M. Yoshimoto, S. Allegrini Jr., J.C. Bressiani, "Tissue response around silicon nitride implants in rabbits", *J. Biomed. Mater. Res. A*, **84** (2008) 337–343.
15. T.J. Webster, A.A. Patel, M.N. Rahaman, B.S. Bal, "Anti-infective and osteointegration properties of silicon nitride, poly(etheretherketone), and titanium implants", *Acta Biomater.*, **8** (2012) 4447–4454.
16. B.S. Bal, M.N. Rahaman, "Orthopedic applications of silicon nitride ceramics", *Acta Biomater.*, **8** (2012) 2889–2898.
17. A. Hoppe, G.B. Nusret, A.R. Boccaccini, "A review of the biological response to ionic dissolution products from bioactive glasses and glass-ceramics", *Biomaterials*, **32** (2011) 2757–2774.
18. A.M. Pietak, J.W. Reid, M.J. Stott, M. Sayer, "Silicon substitution in the calcium phosphate bioceramics", *Biomaterials*, **28** (2007) 4023–4032.
19. V. Mouriño, J.P. Cattalini, A.R. Boccaccini, "Metallic ions as therapeutic agents in tissue engineering scaffolds: An overview of their biological applications and strategies for new developments", *J. R. Soc. Interface*, **9** (2012) 401–419.
20. C. Deng, Q. Yang, X. Sun, L. Chen, C. Feng, J. Chang, C. Wu, "Bioactive scaffolds with Li and Si ions-synergistic effects for osteochondral defects regeneration", *Appl. Mater. Today*, **10** (2018) 203–216.
21. C.C. Guedes-Silva, A.C.D. Rodas, A.C. Silva, C. Ribeiro, F.M.S. Carvalho, O.Z. Higa, T.S. Ferreira, "Microstructure, mechanical properties and in vitro biological behavior of silicon nitride ceramics", *Mater. Res.*, **21** (2018) e20180266.
22. R. Samudrala, A. Azeem, V. Penugurti, B. Manavathi, "Cytocompatibility studies of titania-doped calcium borosilicate bioactive glasses in-vitro", *Mater. Sci. Eng. C*, **77** (2017) 772–779.
23. X. Miao, D. Sun, P.W. Hoo, "Effect of Y-TZP addition on the microstructure and properties of titania-based composites", *Ceram. Int.*, **35** (2009) 281–288.
24. R.C. DeVries, R. Roy, F. Osborn, "Phase equilibria in the system CaO-TiO_2-SiO_2", *J. Am. Ceram. Soc.*, **38** (1955) 158–171.
25. H. Seifert, F. Aldinger, "Phase equilibria in the Si-B-C-N system", pp. 1–58 in *Structure and Bonding*. Ed. M. Jansen, Springer, Berlin, 2002.
26. TOPAS-Academic V5, Coelho Software Brisbane, Australia, http://www.topas-academic.net, 2012.
27. M.D. Abramoff, P.J. Magalhaes, S.J. Ram, "Image processing with ImageJ", *Biophotonics Int.*, **11** (2004) 36–42.
28. G.R., Anstis, P. Chantikul, B.R. Lawn, D.B. Marshall, "A critical evaluation of indentation techniques for measuring fracture toughness: I, Direct crack measurements", *J. Am. Ceram. Soc.*, **64** (1981) 533–542.
29. H. Miyazaki, H. Hyuga, Y. Yoshizawa, K. Hirao, T. Ohji, "Correlation of wear behavior and indentation fracture resistance in silicon nitride ceramics hot-pressed with alumina and yttria", *J. Eur. Ceram. Soc.*, **29** (2009) 1535–1542.
30. A.W. Wren, F.R. Laffir, A. Kidari, M.R. Towler, "The structural role of titanium in Ca-Sr-Zn-Si/Ti glasses for medical applications", *J. Non-Cryst. Solids*, **357** (2011) 1021–1026.
31. Y.F. Kargin, S.N. Ivicheva, A.S. Lysenkov, N.A. Ovsyannikov, L.I. Shvorneva, K.A. Solntsev, "Si_3N_4/TiN composites produced from TiO_2-modified Si_3N_4 powders", *Inorg. Mater.*, **48** (2012) 897–902.
32. A. Bellosi, S. Guicciardi, A. Tampieri, "Development and characterization of electroconductive Si_3N_4-TiN composites", *J. Eur. Ceram. Soc.*, **9** (1992) 83–93.
33. Z.K. Huang, P. Greil, G. Petzow, "Formation of silicon oxinitride from Si_3N_4 and SiO_2 in the presence of Al_2O_3", *Ceram. Int.*, **10** (1984) 14–17.

34. C.C. Guedes-Silva, F.M.S. Carvalho, J.C. Bressiani, "Effect of rare-earth oxides on properties of silicon nitride obtained by normal sintering and sinter-HIP", *J. Rare Earths*, **30** (2012) 1177–1183.
35. L. Gao, J. Li, T. Kusunose, K. Niihara, "Preparation and properties of TiN-Si_3N_4 composites", *J. Eur. Ceram. Soc.*, **24** (2004) 381–386.
36. J. Yan, K.B. Clifton, J.J. Mecholsky Jr., R.L. Reep, "Fracture toughness of manatee rib and bovine femur using a chevron-notched beam test", *J. Biomech.*, **39** (2006) 1066–1074.
37. D. Ćorić, M.M. Renjo, L. Ćurković, "Vickers indentation fracture toughness of Y-TZP dental ceramics", *Int. J. Refract. Metals Hard Mater.*, **64** (2017) 14–19.
38. T. Kokubo, "Bioactive glass ceramics: Properties and applications", *Biomaterials*, **12** (1991) 155–163.
39. R. Zia, M. Riaz, S. Maqsood, S. Anjum, Z. Kayani, T. Hussain, "Titania doped bioactive ceramics prepared by solid state sintering method", *Ceram. Int.*, **41** (2015) 8964–8972.
40. F. Monchau, P. Hivart, B. Genestie, F. Chai, M. Descamps, H.F. Hildebrand, "Calcite as a bone substitute. Comparison with hydroxyapatite and tricalcium phosphate with regard to the osteoblastic activity", *Mater. Sci. Eng. C*, **33** (2013) 490–498.
41. A. Aminian, B. Shirzadi, Z. Azizi, H. Maedler, E. Volkmann, N. Hildebrand, M. Maas, L. Treccani, K. Rezwan, "Enhanced cell adhesion on bioinert ceramics mediated by the osteogenic cell membrane enzyme alkaline phosphatase", *Mater. Sci. Eng. C*, **69** (2016) 184–194.